Deletion of 2-aminoadipic semialdehyde synthase limits metabolite accumulation in cell and mouse models for glutaric aciduria type 1

João Leandro[1,2], Tetyana Dodatko[1,2], Robert J. DeVita[3,4], Hongjie Chen[1,5], Brandon Stauffer[1,5], Chunli Yu[1,5], Sander M. Houten[1,2]

[1]Department of Genetics and Genomic Sciences, Icahn School of Medicine at Mount Sinai, New York, NY 10029, USA
[2]Icahn Institute for Data Science and Genomic Technology, Icahn School of Medicine at Mount Sinai, New York, NY 10029, USA
[3]Department of Pharmacological Sciences, Icahn School of Medicine at Mount Sinai New York, NY 10029, USA
[4]Drug Discovery Institute, Icahn School of Medicine at Mount Sinai, New York, NY 10029, USA
[5]Mount Sinai Genomics, Inc, Stamford, CT 06902, USA

Address for correspondence: Sander Houten, Department of Genetics and Genomic Sciences, Icahn School of Medicine at Mount Sinai, 1425 Madison Avenue, Box 1498, New York, NY 10029, USA. Phone: +1 212 659 9222, Fax: +1 212 659 8754, E-mail: sander.houten@mssm.edu

Short title: Inhibition of AASS in GA1
Word count: 3,919 (Introduction, M&M, Results and Discussion)
Figure count: 4 (with 3 supplemental figures and 4 supplemental tables)
References: 50

This article has been accepted for publication and undergone full peer review but has not been through the copyediting, typesetting, pagination and proofreading process which may lead to differences between this version and the Version of Record. Please cite this article as doi: 10.1002/jimd.12276

Abstract

Glutaric aciduria type 1 (GA1) is an inborn error of lysine degradation characterized by acute encephalopathy that is caused by toxic accumulation of lysine degradation intermediates. We investigated the efficacy of substrate reduction through inhibition of 2-aminoadipic semialdehyde synthase (AASS), an enzyme upstream of the defective glutaryl-CoA dehydrogenase, in a cell line and mouse model of GA1. We show that loss of AASS function in GCDH-deficient HEK-293 cells leads to a ~5-fold reduction in the established GA1 clinical biomarker glutarylcarnitine. In the GA1 mouse model, deletion of *Aass* leads to a 4.3-, 3.8- and 3.2-fold decrease in the glutaric acid levels in urine, brain and liver, respectively. Parallel decreases were observed in urine and brain 3-hydroxyglutaric acid levels, and plasma, urine and brain glutarylcarnitine levels. These *in vivo* data demonstrate that the saccharopine pathway is the main source of glutaric acid production in the brain and periphery of a mouse model for GA1, and support the notion that pharmacological inhibition of AASS may represent an attractive strategy to treat GA1.

Words: 170

Take home message

Inhibition of 2-aminoadipic semialdehyde synthase may represent an attractive strategy to treat glutaric aciduria type 1

Keywords: substrate reduction therapy; glutaric acid; lysine; glutaric aciduria; animal model

Author contributions

Conception and design of the work described: SMH

Acquisition of data: JL, TD, SMH

Analysis and interpretation of data: JL, RJD, HC, BS, CY, SMH

Reporting of the work described: SMH

Guarantor

Sander M. Houten

Ethics statement

All animal experiments were approved by the IACUC of the Icahn School of Medicine at Mount Sinai (# IACUC-2016-0490) and comply with the National Institutes of Health guide for the care and use of Laboratory animals (NIH Publications No. 8023, revised 1978).

Declaration of interests and competing interests

Sander Houten and Robert J. DeVita received funding for this study from Mitsubishi Tanabe Pharma Holdings America.

The authors confirm independence from the sponsors and the content of the article has not been influenced by the sponsors

Introduction

Lysine degradation proceeds mainly via the mitochondrial saccharopine pathway consisting of 9 different enzymatic steps that ultimately yield two acetyl-CoA units and several reduction equivalents (Fig. S1). This pathway is clinically relevant, because defects in two enzymes cause severe inborn errors of metabolism. Pyridoxine-dependent epilepsy (PDE; MIM #266100) is a condition characterized by intractable seizures that can be treated by pyridoxine and lysine-restricted diet. PDE is caused by mutations in *ALDH7A1*.[1,2] Glutaric aciduria type 1 (GA1; MIM #231670) is a cerebral organic aciduria caused by a defect in glutaryl-CoA dehydrogenase (GCDH) encoded by *GCDH* (Fig. S1). GA1 patients can present with macrocephaly and may develop a complex movement disorder due to striatal injury with acute (acute encephalopathic crisis) or insidious onset.[3-6] The accumulation of GCDH substrates, in particular glutaric and 3-hydroxyglutaric acid, is thought to be neurotoxic.[7] GA1 is currently treated by restricting lysine intake, carnitine supplementation and emergency treatment.[8] Remarkably, hyperlysinemia (MIM #238700) and 2-aminoadipic and 2-oxoadipic aciduria (AMOXAD, MIM #204750), two other inborn errors of lysine metabolism, are considered biochemical phenotypes of questionable clinical significance.[9,10] Hyperlysinemia is caused by mutations in *AASS*[11,12], whereas AMOXAD is due to mutations in *DHTKD1*.[13,14]

Substrate reduction therapies for inborn errors of metabolism aim to decrease the levels of toxic metabolite(s) by inhibiting an enzyme upstream of the defective enzyme. The occurrence of seemingly non-harmful enzyme defects in the lysine degradation pathway suggests that substrate reduction therapy by inhibiting these specific enzymes is safe in humans. Accordingly, inhibition of 2-aminoadipic semialdehyde synthase (AASS) has been suggested as a therapeutic intervention in PDE[15,16], but could also work for GA1. Similarly, inhibition of DHTKD1 has been proposed as a therapeutic intervention in GA1.[14,17,18] The latter approach was tested in cell and animal models.[17,18] Unexpectedly, a *Dhtkd1* hypomorph or *Dhtkd1* knock out did not appear to mitigate the clinical and biochemical phenotype of the *Gcdh* KO mouse.[17,18] These results indicate that DHTKD1 is not an exclusive source of glutaryl-CoA, which limits this enzyme's therapeutic potential for substrate reduction to treat GA1.

In our current work, we explore AASS as a target for the treatment of GA1. Based on recent studies, we hypothesize that inhibition of AASS is able to limit flux through the lysine

degradation pathway in liver, kidney, but also the brain.[16,19] AASS is a bifunctional enzyme with two domains, lysine-ketoglutarate reductase (LKR) and saccharopine dehydrogenase (SDH). Most individuals with *AASS* mutations have hyperlysinemia type I due to combined LKR and SDH deficiencies, which is biochemically characterized by hyperlysinemia with no significant or a variable saccharopinuria.[11,12,20,21] Very few cases have been described with hyperlysinemia and a pronounced saccharopinuria due to an isolated SDH defect (hyperlysinemia type II, MIM #268700). Recently reported knockin mouse models clearly illustrate the distinction between type I and type II hyperlysinemia.[22] A model with a missense mutation in the LKR domain equivalent to a variant identified in several type I hyperlysinemia cases (p.R65Q[11]) caused combined LKR and SDH deficiency with no AASS protein expression. These mice had hyperlysinemia without saccharopinuria and no apparent clinical consequences.[22] In contrast, a missense mutation in the SDH domain caused isolated SDH deficiency with accumulation of lysine and saccharopine. These animals displayed liver disease, progressive postnatal growth retardation and died at ~6 weeks of age.[22] Abnormal saccharopine accumulation in worm and mouse models resulted in defective mitochondrial dynamics and function.[22] Therefore, the LKR domain is currently the preferred target for AASS inhibition. Inhibition of LKR is expected to be most similar to hyperlysinemia type I without accumulation of saccharopine.[23] Here, we describe the validation of AASS as a target for the treatment of GA1 in a cell and mouse model.

Material and Methods

Generation of CRISPR-Cas9 Knockout Cell Lines

The generation of gene knockout cell lines using the CRISPR-Cas9 genome editing technique was performed essentially as described[24], with minor modifications.[18,25] Guide and primer sequences are displayed in Table S1.

Immunoblotting

Cells were lysed in RIPA buffer supplemented with protease inhibitor cocktail (Pierce) and centrifuged at 12,000xg, 10 min at 4°C. Frozen mouse tissues (liver and brain) were homogenized in ice-cold RIPA buffer supplemented with protease inhibitor cocktail (~20 mg tissue per 1 mL lysis buffer) using a TissueLyser II apparatus (Qiagen) and the homogenates were centrifuged at 1,000xg, 10 min at 4°C. Total protein was determined using the BCA method. Proteins were separated on a Bolt™ 4–12% Bis-Tris Plus Gel, blotted onto a nitrocellulose membrane and detected using the following primary antibodies: GCDH (gift of Michael Woontner, Children's Hospital Colorado), AASS (Sigma-Aldrich, HPA020728) and citrate synthase [GT1761] (GTX628143, Genetex) or [N2C3] (GTX110624; RRID:AB_1950045, Genetex). Proteins were visualized using IRDye 800CW or IRDye 680RD secondary antibodies (LI-COR, 926-32210; RRID:AB_621842, 926-68070; RRID:AB_10956588, 926-32211; RRID:AB_621843, and 926-68071; RRID:AB_10956166) in an Odyssey CLx Imager (LI-COR) with Image Studio Lite software (version 5.2, LI-COR). Expression of AASS in brain was only detected using a more sensitive chemiluminescence system with an anti-rabbit IgG HRP-linked antibody (Cell Signaling, 7074S, RRID:AB_2099233) and the WesternBright Quantum (Advansta) detection reagent in a FluorChem Q imaging system (Alpha Innotech). Equal loading was checked by Ponceau S staining and the citrate synthase signal.

Acquisition and generation of the mouse models

Gcdh KO (B6.129S4-*Gcdh*^{tm1Dmk}/Mmnc) mice[26] were provided by Dr. Matthew Hirschey (Duke Molecular Physiology Institute, Duke University Medical Center, Durham, NC) after approval of the Mutant Mouse Resource & Research Centers. The *Aass* KO mouse (C57BL/6N-

Aass$^{em1(IMPC)Tcp}$) was created as part of the KOMP2-Phase2 project at The Centre for Phenogenomics (Toronto, ON). It was obtained from the Canadian Mouse Mutant Repository. The *Aass* KO mouse model harbors two CRISPR-Cas9-induced deletions, a 79bp deletion in intron 6, and a 570bp deletion that covers exons 5 and 6, which are both used for genotyping. The *Gcdh* KO model was fully backcrossed to C57BL/6NJ, and the *Aass* KO was generated on the C57BL/6NCrl background. All animal experiments were approved by the IACUC of the Icahn School of Medicine at Mount Sinai (#2016-0490) and comply with the National Institutes of Health guide for the care and use of laboratory animals (NIH Publications No. 8023, revised 1978).

Gcdh and *Aass* KO mice were intercrossed to obtain double heterozygous animals. The double heterozygous mice were then intercrossed to generate mice for the experimental cohort. Breeding pairs using different combinations of *Aass*$^{+/-}$ *Gcdh*$^{+/-}$, *Aass*$^{-/-}$ *Gcdh*$^{+/-}$ and *Aass*$^{+/-}$ *Gcdh*$^{-/-}$ mice were also used to generate mice for the experimental cohort. The experimental cohort consisted of four groups (Table S2). The control group included wild type mice as well as *Aass*$^{+/-}$ and/or *Gcdh*$^{+/-}$ mice. The *Aass* KO group included both *Gcdh*$^{+/+}$ and *Gcdh*$^{+/-}$ mice. The *Gcdh* KO group included both *Aass*$^{+/+}$ and *Aass*$^{+/-}$ mice. Subgroup analysis as well as previous studies demonstrated that *Aass*$^{+/-}$ and *Gcdh*$^{+/-}$ mice are biochemically indistinguishable from wild type mice, which is consistent with the reported recessive mode of inheritance for both traits in humans. The *Gcdh*/*Aass* double KO mice are the final group. All mice were fed a standard rodent chow (PicoLab Rodent Diet 20). Urine of individual mice was collected on multiple days and pooled in order to obtain sufficient sample volume. Mice were euthanized in a random fed state (afternoon) at ~9.4 weeks of age using CO_2. Blood from the inferior vena cava was collected for EDTA plasma isolation, and organs were rapidly excised and snap frozen in liquid nitrogen and subsequently stored at -80ºC.

Metabolite analyses

Quantification of lysine and glutarylcarnitine in HEK-293 cell lines was performed essentially as described previously.[18] Plasma acylcarnitines, plasma amino acids and urine organic acids were measured by the Mount Sinai Biochemical Genetic Testing Lab (now Sema4). Urine creatinine was measured by Jaffe's reaction. Urine organic acids were quantified using a standard curve

and pentadecanoic acid as internal standard. Liver glutaric acid was determined using the same analysis procedure with a homogenate in water containing approximately 10 mg wet weight as matrix. Values were normalized for liver protein content. All animal and metabolite data are available in Table S2.

Brain (half, sagittal, mainly cerebral cortex, no cerebellum, pons and medulla oblongata) samples of 4 females and 3 males from all experimental groups were shipped to Metabolon, Inc. (Research Triangle Park, NC) for global metabolite profiling (mData). For the analysis, proteins were precipitated with methanol followed by centrifugation. The resulting extract was analyzed by two separate reverse phase (RP)/UPLC-MS/MS methods with positive ion mode electrospray ionization (ESI), one RP/UPLC-MS/MS with negative ion mode ESI and by one HILIC/UPLC-MS/MS with negative ion mode ESI essentially as described previously.[27,28] The metabolome data are available in Table S3.

Results

AASS knockout decreases glutarylcarnitine in GCDH-deficient cell lines

In order to obtain proof-of-concept that AASS inhibition can limit metabolite accumulation in GA1, we first used CRISPR-Cas9 genome editing in HEK-293 cells. In order to generate *GCDH*/*AASS* double KO cell lines, we selected three different previously generated *GCDH* single KO cell lines (G1, G7 and G9)[18] and targeted *AASS* in a second round of CRISPR-Cas9 genome editing. Clonal *GCDH*/*AASS* double KO and *AASS* single KO cell lines were selected based on the presence of *AASS* mutations and absent AASS protein in an immunoblot (Figure 1A and B).

We measured cellular lysine and glutarylcarnitine levels in wild type, *GCDH* KO, *AASS* KO and *GCDH*/*AASS* double KO cell lines. For each *GCDH* KO parent clone, a minimum of 4 *GCDH*/*AASS* double KO cell lines were analyzed. Glutarylcarnitine levels were reduced in all 21 *GCDH*/*AASS* double KO cells when compared to the parental *GCDH* single KO cells (Figure 1C). For the individual parental *GCDH* single KO clones, the average observed reduction in glutarylcarnitine was 4.7-, 2.1-, 6.2- and 5.4-fold in *GCDH*/*AASS* double KO cell lines (Figure 1C). The less pronounced decrease in the *GCDH*/*AASS* double KO cell lines derived from the G7 *GCDH* single KO cell line (2.1-fold) were due to the smaller elevation of glutarylcarnitine before *AASS* KO. Differences between clones are sometimes observed in these CRISPR-Cas9 experiments and may be artifacts related to differences in cell growth rate after clonal expansion. Cellular lysine levels did not increase upon *AASS* KO (Figure 1C). We also noted a 1.7-fold decrease in the glutarylcarnitine levels of *AASS* single KO cells (Figure 1D). Consistent with the results in the *GCDH*/*AASS* double KO cell lines lysine levels also did not change in the *AASS* single KO cells (Figure 1D).

Validation of the Aass KO mouse line

Cell line models inaccurately represent the complex physiology of lysine degradation in vivo. We therefore studied the consequence of *Aass* KO in a mouse model. The *Aass* KO mouse employed in this study has not yet been reported in the literature. The mutant allele is expected to be a true loss-of-function allele with a loss of both LKR and SDH activities, which is

biochemically equivalent to complete inhibition of LKR. Indeed, the plasma concentration of lysine was elevated in *Aass* KO mice when compared to *Aass*$^{+/-}$ and wild type animals. AASS protein levels in liver and brain were absent in the KO animals (Figure S2). Importantly, we observed a prominent decrease of plasma 2-aminoadipic acid in *Aass* KO mice, which indicates that flux through the lysine degradation pathway is indeed impaired by loss of AASS function (Figure S2). *Aass* KO mice appeared healthy and developed normally, which is consistent with the findings in a mouse model for hyperlysinemia comparable to our model.[22] In addition, no significant phenotypes are reported on the International Mouse Phenotyping Consortium (IMPC) website.

Generation and characterization of Gcdh/Aass double KO mice

In order to generate an experimental cohort, we intercrossed *Gcdh*/*Aass* double heterozygous mice. The genotype distribution in the progeny (85 pups) was not Mendelian with a shortage of *Gcdh* KO mice (Table S4). All different *Aass* genotypes were present within the *Gcdh* KO group. *Aass* KO mice were overrepresented in this cross. Previously, heterozygote mating of *Gcdh*$^{+/-}$ mice on a mixed background (129/SvJ X C57BL/6J) has been reported to yield the expected Mendelian genotype distribution indicating that *Gcdh* KO mice have normal fetal and post-natal viability.[26] Therefore, this aberrant genotype distribution is either a false positive that will disappear upon generation of more progeny, or a true effect caused by the congenic C57BL/6 background of this cohort. *Gcdh*/*Aass* double KO mice appeared healthy and developed normally. As reported by others[26], kidney weight was increased in *Gcdh* KO mice, but normalized in *Gcdh*/*Aass* double KO mice (Table S2).

Glutaric aciduria in Gcdh KO mice is decreased in Gcdh/Aass double KO mice

We first studied the main diagnostic markers of GA1 (Table S2). Glutaric acid is the major accumulating metabolite in urine of *Gcdh* KO mice and was ~450-fold higher when compared to urine from control animals (Figure 2). Glutaric acid in *Gcdh*/*Aass* double KO mice was 4.3-fold lower than in *Gcdh* KO mice (Figure 2). 3-Hydroxyglutaric acid is the pathognomonic marker for GA1 (Figure 2). The excretion of 3-hydroxyglutaric acid was 1.7-fold lower in *Gcdh*/*Aass* double KO mice when compared to *Gcdh* KO mice (Figure 2). Glutarylcarnitine excretion was 2.9-fold

lower in *Gcdh*/*Aass* double KO mice (Figure 2). The plasma concentration of glutarylcarnitine, an important diagnostic marker, was decreased 2.8-fold in *Gcdh*/*Aass* double KO mice when compared to *Gcdh* KO mice (Figure 3). We conclude that the urinary excretion of glutaryl-CoA derived metabolites in *Gcdh* KO mice is significantly reduced by deletion of *Aass*.

Other selected plasma and urine metabolites

Plasma free carnitine concentration was lower in *Gcdh* KO mice when compared to controls, which is likely a reflection of the sequestration of free carnitine as glutarylcarnitine. As a result of this secondary carnitine deficiency, many short-chain acylcarnitines are decreased in *Gcdh* KO mice. Carnitine and short-chain acylcarnitine concentrations normalized in *Gcdh*/*Aass* double KO mice (Figure 3, Table S2).

Plasma lysine concentration was increased in *Aass* KO and *Gcdh*/*Aass* double KO mice, and did not differ between these groups (Figure 3). Homocitrulline, a known biochemical marker for hyperlysinemia, was also elevated in both groups (Figure 3). The concentration of 2-aminoadipic acid was 1.8-fold increased in *Gcdh* KO mice when compared to controls, which is consistent with our previous work.[18] KO of *Aass* in the *Gcdh* KO animals led to a 5.7-fold decrease in the concentration of 2-aminoadipic acid (Figure 3). Urine 2-oxoadipic acid was increased 1.7-fold in *Gcdh* KO mice when compared to controls, again consistent with our previous work.[18] KO of *Aass* in the *Gcdh* KO animals led to a 2.4-fold decrease in urinary excretion of 2-oxoadipic acid (Figure 2). Combined, these changes in the plasma amino acid and urine organic acid profiles are consistent with decreased flux through the lysine degradation pathway in mice lacking AASS.

The urine amino acid profile of *Aass* KO and *Gcdh*/*Aass* double KO mice indicated urinary loss of several amino acids (Figure 2, Table S2). Ranked based on their elevation, these amino acids are: lysine, homocitrulline, arginine, citrulline, cystine, ornithine, mixed disulphide of cysteine and homocysteine, cystathionine, hydroxylysine, glutamine and leucine. This is consistent with competitive inhibition of the dibasic amino acid transporters SLC7A7 and SLC7A9/SLC3A1 in kidney by the high urine lysine levels leading to an amino aciduria that biochemically resembles a combination of lysinuric protein intolerance and cystinuria.[20,29]

Glutaric acid accumulation in Gcdh KO brain is decreased in Gcdh/Aass double KO mice

Global metabolic profiles were determined in brain samples from all 4 groups of mice (Figure 4, Table S3). Glutaric acid levels were increased 181-fold in *Gcdh* KO brain when compared to controls. KO of *Aass* in the *Gcdh* KO animals led to a 3.8-fold decrease in glutaric acid. Glutarylcarnitine and 3-hydroxyglutaric acid were increased 39.0- and 2.3-fold in *Gcdh* KO brain, and were decreased 1.5- and 1.6-fold in *Gcdh*/*Aass* double KO brain, respectively. The levels of 2-aminoadipic acid were increased 1.6-fold in *Gcdh* KO brain, and decreased 12.9-fold in *Gcdh*/*Aass* double KO brain to a similar level as observed in *Aass* KO brain. Lysine and several derivatives such as pipecolate, homoarginine, homocitrulline, N6-acetyllysine and N2-acetyllysine, were elevated in *Aass* KO and *Gcdh*/*Aass* double KO brain. Saccharopine was not detected in any of the *Aass* KO and *Gcdh*/*Aass* double KO brains. We conclude that the levels of glutaryl-CoA derived metabolites in *Gcdh* KO brain are significantly reduced by deletion of *Aass*.

In order to be able to compare brain with other tissues, we measured glutaric acid levels in liver. Glutaric acid levels in *Gcdh* KO liver were very similar to previously reported values[30,31] and decreased 3.2-fold upon *Aass* inactivation (Fig. S3). Overall, the decrease in glutaric acid in liver was comparable with brain and urine.

Discussion

GA1 is a harmful condition for which therapeutic options should be further improved. We investigated the potential of substrate reduction through inhibition of AASS, an enzyme upstream of the defective GCDH, in a cell line and mouse model of GA1. We show that loss of *AASS* in GCDH-deficient HEK-293 cells leads to a significant decrease in the established GA1 clinical biomarker glutarylcarnitine. In the GA1 mouse model, deletion of *Aass* leads to a 4.3-, 3.8-, and 3.2-fold decrease in the glutaric acid levels in urine, brain and liver, respectively. Parallel decreases were observed in urine and brain 3-hydroxyglutaric acid levels, and plasma, urine and brain glutarylcarnitine levels. These cell line and mouse data demonstrate that the saccharopine pathway is the main source of GCDH substrates in a human cell line and the brain and periphery of a mouse model for GA1, and support the notion that pharmacological inhibition of AASS may represent an attractive strategy to treat GA1.

A limitation of our work is that we only studied the GA1 mouse on a regular chow diet containing 1.17% lysine. Under these conditions, the GA1 mouse has a pronounced biochemical phenotype, but limited clinical consequences.[26] Exposure to elevated dietary protein or lysine is necessary to induce a neurological phenotype that resembles human GA1 with seizures, paralysis, subarachnoidal hemorrhages and death.[32] Future studies will have to evaluate if *Aass* KO can prevent this diet-induced neurological phenotype. A second caveat of our study is that an LKR inhibitor will likely not lead to full blockage of the enzyme and is therefore not directly comparable to the *Aass* KO mouse model. The flux control exerted by LKR over lysine catabolism is currently unknown, but a 50% reduction in AASS protein is apparently without metabolic consequences. The future discovery of highly potent AASS inhibitors will enable metabolic control studies that are needed to address this issue. In addition, and as detailed below, a useful LKR inhibitor will need to be able to cross the blood-brain barrier.

In the mouse studies, the most pronounced decrease was observed for the levels of glutaric acid. Glutaric acid is the major metabolite excreted in GA1 patients and the *Gcdh* KO mouse. In the mouse model, the urinary excretion of glutaric acid is 32-fold and 359-fold higher than that of 3-hydroxyglutaric acid and glutarylcarnitine, respectively. Thus, of the alternative pathways for glutaryl-CoA metabolism, the conversion to glutaric acid, which may be mediated by a thiolase or occur non-enzymatically, has the highest capacity. The conversion to 3-

hydroxyglutaric acid proceeds via glutaconyl-CoA and 3-hydroxyglutaryl-CoA and depends on 3-methylglutaconyl-CoA hydratase and medium-chain acyl-CoA dehydrogenase.[33,34] The formation of glutarylcarnitine depends on carnitine availability[30] and an as of yet unknown carnitine acyltransferase. Carnitine supplementation enhances the formation of glutarylcarnitine, but does not affect the accumulation of glutaric acid in brain, liver, kidney and serum.[30] The relatively small decreases in the production of 3-hydroxyglutaric acid and glutarylcarnitine upon *Aass* deletion indicate that these pathways are saturated in the *Gcdh* KO mouse. The metabolite accumulation in *Gcdh* KO and GA1 brain shows a pattern similar to urine, with the accumulation of glutaric acid higher than the accumulation of 3-hydroxyglutaric acid and glutarylcarnitine.[7,30-32,35,36] The *Aass* KO led to a pronounced 3.8-fold decrease in brain glutaric acid level, with smaller changes in glutarylcarnitine and 3-hydroxyglutaric acid (1.5- and 1.6-fold, respectively). These data demonstrate that deletion of *Aass* in the GA1 mouse model mainly affects the accumulation of glutaric acid.

Our results align well with a previous study in which the effect of low lysine diets was evaluated in *Gcdh* KO mice.[30] Decreasing lysine intake by changing from standard diet (1.7% (w/w) L-lysine) to diets containing 0.4, 0.2 and 0.1% lysine led to a pronounced decrease in brain and liver glutaric acid with only minimal or no changes in 3-hydroxyglutaric acid and glutarylcarnitine.[30] Our results also mimic the reported biochemical response to dietary treatment in GA1 patients.[37-41] In their description of a larger patient cohort, Hoffmann and colleagues report that dietary therapy reduced urinary excretion of glutaric acid by ~4.3-fold (77%).[42,43]

We show that the accumulation of metabolites derived from glutaryl-CoA decreased upon AASS inactivation, but did not reach control levels. It is well known that AASS is not a unique source of GCDH substrates, because the degradation of hydroxylysine and tryptophan feed into the lysine degradation pathway by producing 2-aminoadipic acid 6-semialdehyde and 2-oxoadipic acid, respectively (Fig. S1). It is thought, however, that the accumulation of glutaric acid in the brain is mostly due to lysine degradation within the brain.[31] This is corroborated by the fact that all genes known to function in the lysine degradation pathway are well expressed in the relevant brain areas such as the putamen and caudate.[44] Therefore dietary treatment of GA1 patients is aimed to minimize the transfer of lysine across the blood-brain barrier. It has

been suggested that in the brain the initial steps in lysine degradation proceed via α-deamination and the formation of pipecolate rather than via ε-deamination and the formation of saccharopine mediated by AASS (Fig. S1).[30,45] Indeed, the increased levels of pipecolate in *Aass* KO brain argue in favor of lysine degradation via α-deamination, and are consistent with the reported increased excretion of pipecolate in individuals with hyperlysinemia.[46] Recent work, however, suggested that also in mouse brain, human astrocytes and a human neural progenitor cell line, the AASS-mediated pathway is the main route for lysine degradation.[16,19] Using stable isotope labeling, multiple studies have demonstrated that pipecolate formed via lysine α-deamination does not significantly contribute to the production of 2-aminoadipic acid.[16,19,47] Our work now provides genetic evidence that the AASS-mediated pathway is indeed the main source of GCDH substrates in the brain of GA1 mice. We can, however, not exclude the possibility that lysine degradation via α-deamination is responsible for some of the remaining accumulation of glutaryl-CoA derived metabolites. Our conclusions are based on a thorough evaluation of steady-state metabolite levels in urine, plasma, brain and liver. Follow-up studies in these new animal models should include stable isotope tracer approaches with labeled lysine to estimate glutaric acid production rates.

Hyperlysinemia is considered a biochemical phenotype of questionable clinical significance.[10] Our hyperlysinemia mouse model recapitulates the biochemical abnormalities observed in hyperlysinemia cases. These include increased levels of lysine, pipecolate, homocitrulline, homoarginine, N-ε-acetyl-L-lysine, N-α-acetyl-L-lysine, gamma-glutamyl-α-lysine and gamma-glutamyl-ε-lysine. We noted that hyperlysinemia due to *Aass* KO led to a consistent dibasic amino aciduria. A similar phenomenon has been observed in patients with hyperlysinemia ("intermittent cystinuria").[20,29] The cystine concentration in *Aass* KO urine surpassed the reported upper limit of solubility (1.25 mmol/L at pH 7.5). We observed fluid in the kidney of 2 out of 17 *Aass* KO mice, but have not systematically studied kidney or bladder cystine stones. The increased excretion of cystathionine was unexpected, but has been reported in cystinuria.[48-50] No other major phenotypes were observed in the *Aass* KO mice.

In summary, our data demonstrate that the saccharopine pathway is the main source of glutaric acid production in the brain and periphery of a mouse model for GA1. We argue that

substrate reduction therapy by inhibition of AASS should be further explored as a treatment option for GA1, but also PDE.

Acknowledgments

We thank Dr. Jonna Westover (University of Utah), Dr. Frank Frerman (University of Colorado) and Dr. Michael Woontner (Children's Hospital Colorado) for providing the anti-GCDH antibody, Dr. Matthew Hirschey for providing the *Gcdh* KO mice, and Dr. Nolan Skop (Mount Sinai Innovation Partners) for development and maintenance of external partnerships. We thank Purvika Patel for excellent technical assistance with the clinical biochemical analyses. Research reported in this publication was supported by a sponsored research agreement with Mitsubishi Tanabe Pharma Holdings America.

References

1. Mills PB, Struys E, Jakobs C, et al. Mutations in antiquitin in individuals with pyridoxine-dependent seizures. *Nat.Med.* 2006;12(3):307-309.
2. van Karnebeek CD, Tiebout SA, Niermeijer J, et al. Pyridoxine-Dependent Epilepsy: An Expanding Clinical Spectrum. *Pediatr Neurol* 2016;596-12.
3. Harting I, Neumaier-Probst E, Seitz A, et al. Dynamic changes of striatal and extrastriatal abnormalities in glutaric aciduria type I. *Brain* 2009;132(Pt 7):1764-1782.
4. Greenberg CR, Reimer D, Singal R, et al. A G-to-T transversion at the +5 position of intron 1 in the glutaryl CoA dehydrogenase gene is associated with the Island Lake variant of glutaric acidemia type I. *Hum Mol Genet* 1995;4(3):493-495.
5. Goodman SI, Stein DE, Schlesinger S, et al. Glutaryl-CoA dehydrogenase mutations in glutaric acidemia (type I): review and report of thirty novel mutations. *Hum Mutat* 1998;12(3):141-144.
6. Boy N, Garbade SF, Heringer J, et al. Patterns, evolution, and severity of striatal injury in insidious- versus acute-onset glutaric aciduria type 1. *J Inherit Metab Dis* 2019;42(1):117-127.
7. Funk CB, Prasad AN, Frosk P, et al. Neuropathological, biochemical and molecular findings in a glutaric acidemia type 1 cohort. *Brain* 2005;128(Pt 4):711-722.
8. Boy N, Muhlhausen C, Maier EM, et al. Proposed recommendations for diagnosing and managing individuals with glutaric aciduria type I: second revision. *J Inherit Metab Dis* 2017;40(1):75-101.
9. Dancis J, Hutzler J, Ampola MG, et al. The prognosis of hyperlysinemia: an interim report. *Am. J. Hum. Genet.* 1983;35(3):438-442.
10. Goodman SI & Duran M. in *Physician's guide to the diagnosis, treatment, and follow-up of inherited metabolic diseases* (eds N. Blau, M. Duran, K.M. Gibson, & C. Dionisi-Vici) 691-705 (Springer Verlag, 2014).
11. Houten SM, te Brinke H, Denis S, et al. Genetic basis of hyperlysinemia. *Orphanet J. Rare Dis.* 2013;857.
12. Sacksteder KA, Biery BJ, Morrell JC, et al. Identification of the alpha-aminoadipic semialdehyde synthase gene, which is defective in familial hyperlysinemia. *Am. J. Hum. Genet.* 2000;66(6):1736-1743.
13. Hagen J, te Brinke H, Wanders RJ, et al. Genetic basis of alpha-aminoadipic and alpha-ketoadipic aciduria. *J Inherit Metab Dis* 2015;38(5):873-879.
14. Danhauser K, Sauer SW, Haack TB, et al. DHTKD1 Mutations Cause 2-Aminoadipic and 2-Oxoadipic Aciduria. *Am J Hum Genet* 2012;91(6):1082-1087.
15. Pena IA, MacKenzie A & Van Karnebeek CDM. Current knowledge for pyridoxine-dependent epilepsy: a 2016 update. *Expert Review of Endocrinology & Metabolism* 2017;12(1):5-20.
16. Pena IA, Marques LA, Laranjeira AB, et al. Mouse lysine catabolism to aminoadipate occurs primarily through the saccharopine pathway; implications for pyridoxine dependent epilepsy (PDE). *Biochim Biophys Acta* 2017;1863(1):121-128.
17. Biagosch C, Ediga RD, Hensler SV, et al. Elevated glutaric acid levels in Dhtkd1-/Gcdh-double knockout mice challenge our current understanding of lysine metabolism. *Biochim Biophys Acta* 2017;1863(9):2220-2228.

18. Leandro J, Dodatko T, Aten J, et al. DHTKD1 and OGDH display substrate overlap in cultured cells and form a hybrid 2-oxo acid dehydrogenase complex in vivo. *Hum Mol Genet* 2020;29(7):1168–1179.
19. Crowther LM, Mathis D, Poms M & Plecko B. New insights into human lysine degradation pathways with relevance to pyridoxine dependent epilepsy due to antiquitin deficiency. *J Inherit Metab Dis* 2019;42(4):620-628.
20. Cederbaum SD, Shaw KN, Dancis J, Hutzler J & Blaskovics JC. Hyperlysinemia with saccharopinuria due to combined lysine-ketoglutarate reductase and saccharopine dehydrogenase deficiencies presenting as cystinuria. *J.Pediatr.* 1979;95(2):234-238.
21. Tondo M, Calpena E, Arriola G, et al. Clinical, biochemical, molecular and therapeutic aspects of 2 new cases of 2-aminoadipic semialdehyde synthase deficiency. *Mol Genet Metab* 2013;110(3):231-236.
22. Zhou J, Wang X, Wang M, et al. The lysine catabolite saccharopine impairs development by disrupting mitochondrial homeostasis. *J Cell Biol* 2019;218(2):580-597.
23. Leandro J & Houten SM. Saccharopine, a lysine degradation intermediate, is a mitochondrial toxin. *J Cell Biol* 2019;218(2):391-392.
24. Ran FA, Hsu PD, Wright J, et al. Genome engineering using the CRISPR-Cas9 system. *Nat Protoc* 2013;8(11):2281-2308.
25. Violante S, Achetib N, van Roermund CWT, et al. Peroxisomes can oxidize medium- and long-chain fatty acids through a pathway involving ABCD3 and HSD17B4. *FASEB J* 2019;33(3):4355-4364.
26. Koeller DM, Woontner M, Crnic LS, et al. Biochemical, pathologic and behavioral analysis of a mouse model of glutaric acidemia type I. *Hum Mol Genet* 2002;11(4):347-357.
27. Miller MJ, Kennedy AD, Eckhart AD, et al. Untargeted metabolomic analysis for the clinical screening of inborn errors of metabolism. *J Inherit Metab Dis* 2015;38(6):1029-1039.
28. Evans AM, Bridgewater BR, Miller LAD, et al. High resolution mass spectrometry improves data quantity and quality as compared to unit mass resolution mass spectrometry in high-throughput profiling metabolomics. *Metabolomics* 2014;4132.
29. Ozalp I, Hasanoglu A, Tuncbilek E & Yalaz K. Hyperlysinemia without clinical findings. *Acta Paediatr Scand* 1981;70(6):951-953.
30. Sauer SW, Opp S, Hoffmann GF, et al. Therapeutic modulation of cerebral L-lysine metabolism in a mouse model for glutaric aciduria type I. *Brain* 2011;134(Pt 1):157-170.
31. Sauer SW, Okun JG, Fricker G, et al. Intracerebral accumulation of glutaric and 3-hydroxyglutaric acids secondary to limited flux across the blood-brain barrier constitute a biochemical risk factor for neurodegeneration in glutaryl-CoA dehydrogenase deficiency. *J Neurochem* 2006;97(3):899-910.
32. Zinnanti WJ, Lazovic J, Wolpert EB, et al. A diet-induced mouse model for glutaric aciduria type I. *Brain* 2006;129(Pt 4):899-910.
33. Mack M, Schniegler-Mattox U, Peters V, et al. Biochemical characterization of human 3-methylglutaconyl-CoA hydratase and its role in leucine metabolism. *The FEBS journal* 2006;273(9):2012-2022.

34. Peters V, Morath M, Mack M, et al. Formation of 3-hydroxyglutaric acid in glutaric aciduria type I: in vitro participation of medium chain acyl-CoA dehydrogenase. *JIMD Rep* 2019;47(1):30-34.
35. Zinnanti WJ, Lazovic J, Housman C, et al. Mechanism of age-dependent susceptibility and novel treatment strategy in glutaric acidemia type I. *J Clin Invest* 2007;117(11):3258-3270.
36. Sauer SW, Opp S, Komatsuzaki S, et al. Multifactorial modulation of susceptibility to l-lysine in an animal model of glutaric aciduria type I. *Biochim Biophys Acta* 2015;1852(5):768-777.
37. Yamaguchi S, Orii T, Yasuda K & Kohno Y. A case of glutaric aciduria type I with unique abnormalities in the cerebral CT findings. *Tohoku J Exp Med* 1987;151(3):293-299.
38. Brandt NJ, Gregersen N, Christensen E, Gron IH & Rasmussen K. Treatment of glutaryl-CoA dehydrogenase deficiency (glutaric aciduria). Experience with diet, riboflavin, and GABA analogue. *J Pediatr* 1979;94(4):669-673.
39. Bennett MJ, Marlow N, Pollitt RJ & Wales JK. Glutaric aciduria type 1: biochemical investigations and postmortem findings. *European journal of pediatrics* 1986;145(5):403-405.
40. Whelan DT, Hill R, Ryan ED & Spate M. L-Glutaric acidemia: investigation of a patient and his family. *Pediatrics* 1979;63(1):88-93.
41. Goodman SI, Markey SP, Moe PG, Miles BS & Teng CC. Glutaric aciduria; a "new" disorder of amino acid metabolism. *Biochem Med* 1975;12(1):12-21.
42. Hoffmann GF, Trefz FK, Barth PG, et al. Glutaryl-coenzyme A dehydrogenase deficiency: a distinct encephalopathy. *Pediatrics* 1991;88(6):1194-1203.
43. Hoffmann GF, Athanassopoulos S, Burlina AB, et al. Clinical course, early diagnosis, treatment, and prevention of disease in glutaryl-CoA dehydrogenase deficiency. *Neuropediatrics* 1996;27(3):115-123.
44. GTEx Consortium. Human genomics. The Genotype-Tissue Expression (GTEx) pilot analysis: multitissue gene regulation in humans. *Science* 2015;348(6235):648-660.
45. Hallen A, Jamie JF & Cooper AJ. Lysine metabolism in mammalian brain: an update on the importance of recent discoveries. *Amino Acids* 2013;45(6):1249-1272.
46. Woody NC & Pupene MB. Excretion of pipecolic acid by infants and by patients with hyperlysinemia. *Pediatr.Res.* 1970;4(1):89-95.
47. Posset R, Opp S, Struys EA, et al. Understanding cerebral L-lysine metabolism: the role of L-pipecolate metabolism in Gcdh-deficient mice as a model for glutaric aciduria type I. *J Inherit Metab Dis* 2015;38(2):265-272.
48. Frimpter GW. Cystathioninuria in a patient with cystinuria. *Am J Med* 1969;46(5):832-836.
49. Strickler JC & Frimpter GW. Renal excretion of cystathionine in dogs. *Am J Physiol* 1969;217(4):1199-1204.
50. Hoppe A, Denneberg T, Jeppsson JO & Kagedal B. Urinary excretion of amino acids in normal and cystinuric dogs. *Br Vet J* 1993;149(3):253-268.

Figure legends

Figure 1. Characterization of *GCDH*/*AASS* double KO cell lines. (A and B) Immunoblot validation of *GCDH*/*AASS* double KO cell lines (A) and of *AASS* single KO cell lines (B). Three *GCDH* KO clones (G1, G7 and G9) were selected for the generation of the *GCDH*/*AASS* double KO cell lines. *AASS* KO cell lines were generated in wild type HEK-293 cells. Citrate synthase (CS) was used as loading control and the position of molecular mass marker proteins (in kDa) is given. (C) Analysis of glutarylcarnitine and lysine in the *GCDH*/*AASS* double KO cell lines (△), the parental *GCDH* single KO cell lines (■) and wild type HEK-293 cells (○). Single *GCDH* KO clones are indicated as G# and double *GCDH*/*AASS* KO clones as G#A#. (D) Analysis of glutarylcarnitine and lysine in *AASS* single KO cell lines (▼) and wild type HEK-293 cells (○). Error bars indicate SD.

Figure 2. Urine metabolite levels in control, *Aass* KO, *Gcdh* KO and *Aass*/*Gcdh* double KO animals. ND, not detected. Error bars indicate SD. The P value for the ANOVA was < 0.0001 for all displayed metabolites. A Tukey's multiple comparisons test was performed to compare the mean of each group with the mean of every other group. The result is only displayed for the *Aass*/*Gcdh* double KO versus *Gcdh* KO comparison. ****, P < 0.0001.

Figure 3. Plasma metabolite concentrations in control, *Aass* KO, *Gcdh* KO and *Aass*/*Gcdh* double KO animals. Error bars indicate SD. The P value for the ANOVA was 0.0143 for carnitine and < 0.0001 for all other displayed metabolites. A Tukey's multiple comparisons test was performed to compare the mean of each group with the mean of every other group. The result is only displayed for the *Aass*/*Gcdh* double KO versus *Gcdh* KO comparison. *, P < 0.05; **, P < 0.01; ***, P < 0.001; ****, P < 0.0001.

Figure 4. Brain metabolite levels in control, *Aass* KO, *Gcdh* KO and *Aass*/*Gcdh* double KO animals. The scaled imputed data (ScaledImpData) represent the normalized raw area counts of each metabolite rescaled to set the median equal to 1. Any missing values are imputed with the minimum (2/7 glutarate values and 7/7 glutarylcarnitine values in the *Aass* KO group). The

experimental groups consisted of 4 females and 3 males. No obvious effect of sex was observed, except for pipecolate, which was consistently higher in the male mice. Error bars indicate SD. The P value for the ANOVA was < 0.0001 for all displayed metabolites. A Tukey's multiple comparisons test was performed to compare the mean of each group with the mean of every other group. The result is only displayed for the *Aass*/*Gcdh* double KO versus *Gcdh* KO comparison. ***, P < 0.001; ****, P < 0.0001.

Supplemental Figure legends

Figure S1. The lysine degradation pathway. The degradation of L-lysine may occur via two pathways: the saccharopine and the pipecolate pathway. The mitochondrial saccharopine pathway is well established and is the major pathway. It consists of nine different enzymatic steps that ultimately yield 2 acetyl-CoAs and several reducing equivalents. The pipecolate pathway, which is thought to be more active in the brain, proceeds via oxidative α-deamination with L-pipecolate as intermediate. Degradation of L-hydroxy-L-lysine leads to L-2-aminoadipic acid 6-semialdehyde and cytosolic degradation of tryptophan with kynurenine as intermediate leads to the production of 2-oxoadipic ac1d (OA). The intermediate OA is metabolized into glutaryl-CoA via oxidative decarboxylation by the DHTKD1, the E1 subunit of the 2-oxoadipic acid dehydrogenase complex (OADHc). Glutaryl-CoA is converted into crotonyl-CoA via oxidative decarboxylation by GCDH. The GCDH protein is deficient in GA1 leading to the accumulation of glutaryl-CoA metabolites: glutarylcarnitine (C5DC), glutaric acid and 3-hydroxyglutaric acid. The level of 2-aminoadipic acid (AA) correlates with the amount of OA by reversible transamination catalyzed by AADAT. C5DC is the product of detoxification of accumulating glutaryl-CoA through conjugation with carnitine. AASS, 2-aminoadipic semialdehyde synthase; ALDH7A1, 2-aminoadipic semialdehyde dehydrogenase; AADAT, kynurenine/2-aminoadipate aminotransferase; CRYM/KR, μ-crystallin/ketimine reductase; DHTKD1, dehydrogenase E1 and transketolase domain containing 1; GCDH, glutaryl-CoA dehydrogenase; ECHS1, enoyl-CoA hydratase; HADH, hydroxyacyl-coenzyme A dehydrogenase; ACAA2, acetyl-CoA acyltransferase 2; P5CR, pyrroline-5-carboxylate reductase; PIPOX, peroxisomal sarcosine oxidase; HYKK, hydroxylysine kinase; PHYKPL, 5-phosphohydroxy-L-lysine phospho-lyase. Dashed arrows represent not fully characterized enzymatic steps.

Figure S2. Concentration of lysine and 2-aminoadipic acid in plasma, and AASS protein level in liver and brain of *Aass* KO and a combination of *Aass*$^{+/-}$ and wild type mice. Citrate synthase (CS) was used as loading control in the immunoblot.

Figure S3. Liver glutaric acid levels in control, *Aass* KO, *Gcdh* KO and *Aass*/*Gcdh* double KO animals. Glutaric acid was essentially undetectable in control and *Aass* KO samples. Error bars indicate SD. The P value for the ANOVA was < 0.0001 for all displayed metabolites. A Tukey's multiple comparisons test was performed to compare the mean of each group with the mean of every other group. The result is only displayed for the *Aass*/*Gcdh* double KO versus *Gcdh* KO comparison. ****, P < 0.0001.

Supplemental tables

Table S1. Guide sequences used for the CRISPR-Cas9 targeting, and primers for PCR amplification and Sanger sequencing.

Table S2. All animal and metabolite data collected in this study.

Table S3. The results of the metabolome profiling displayed as a heat map of statistically significant biochemicals profiled in this study.

Table S4. The genotype distribution in a cross of *Gcdh*$^{+/-}$/*Aass*$^{+/-}$ X *Gcdh*$^{+/-}$/*Aass*$^{+/-}$ mice.

Figure 1

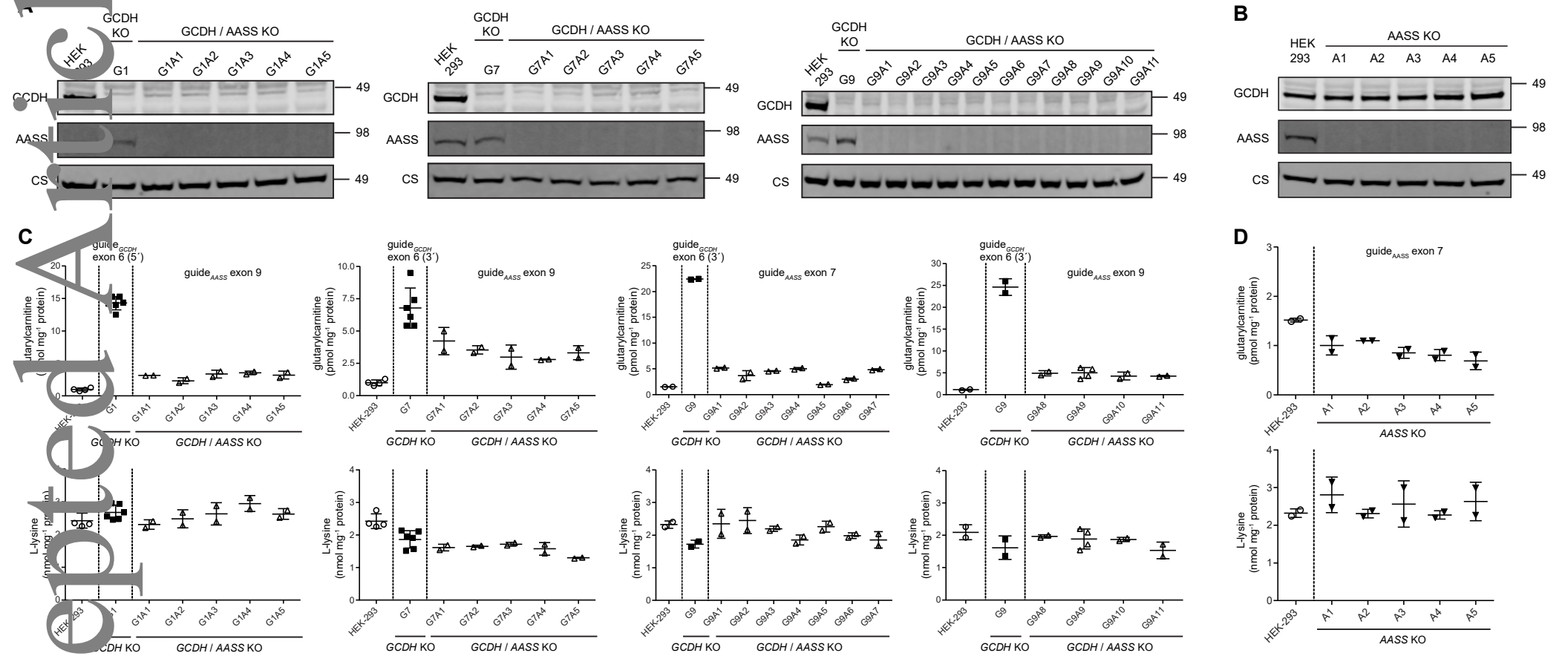

Figure 2

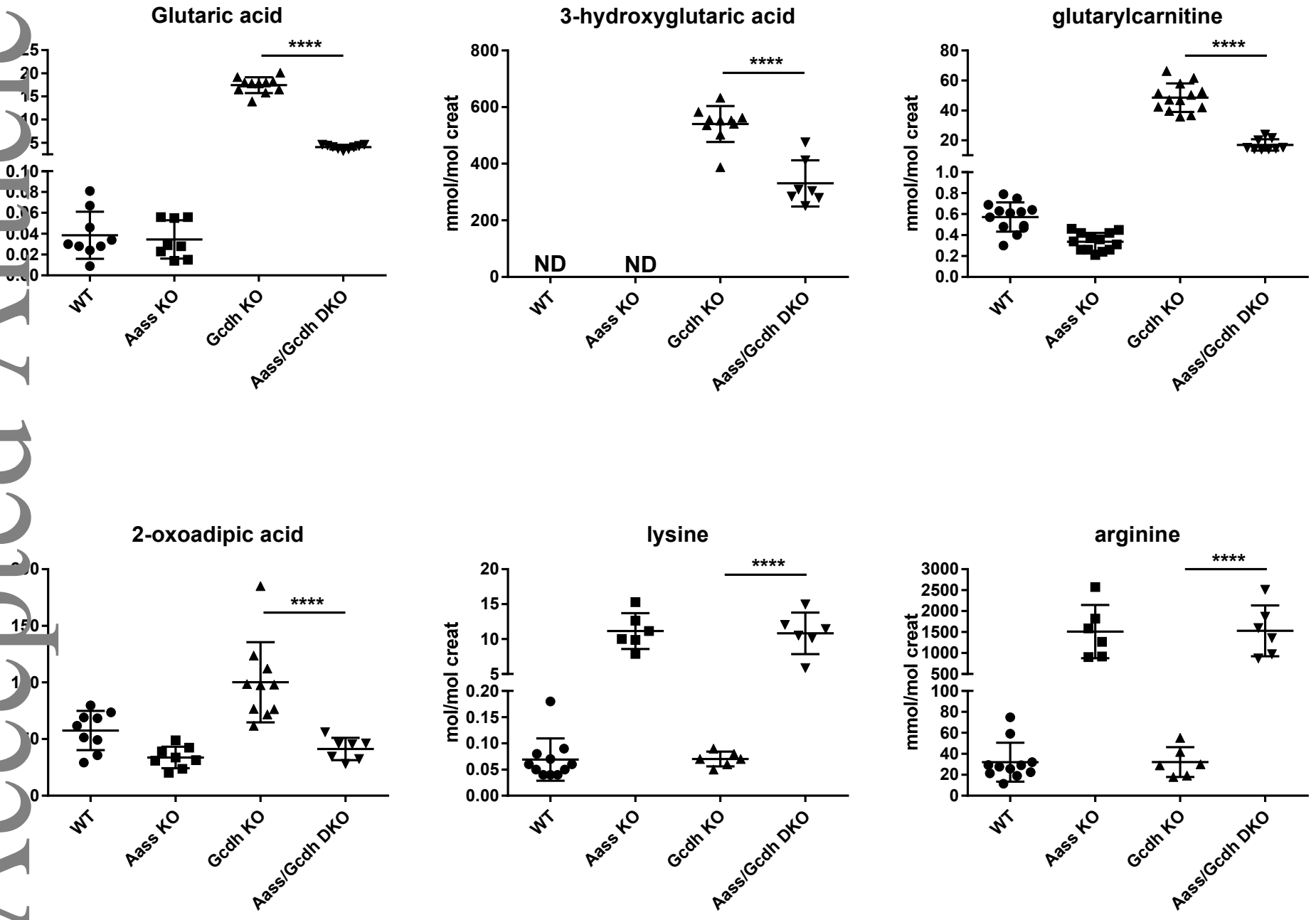

Figure 3

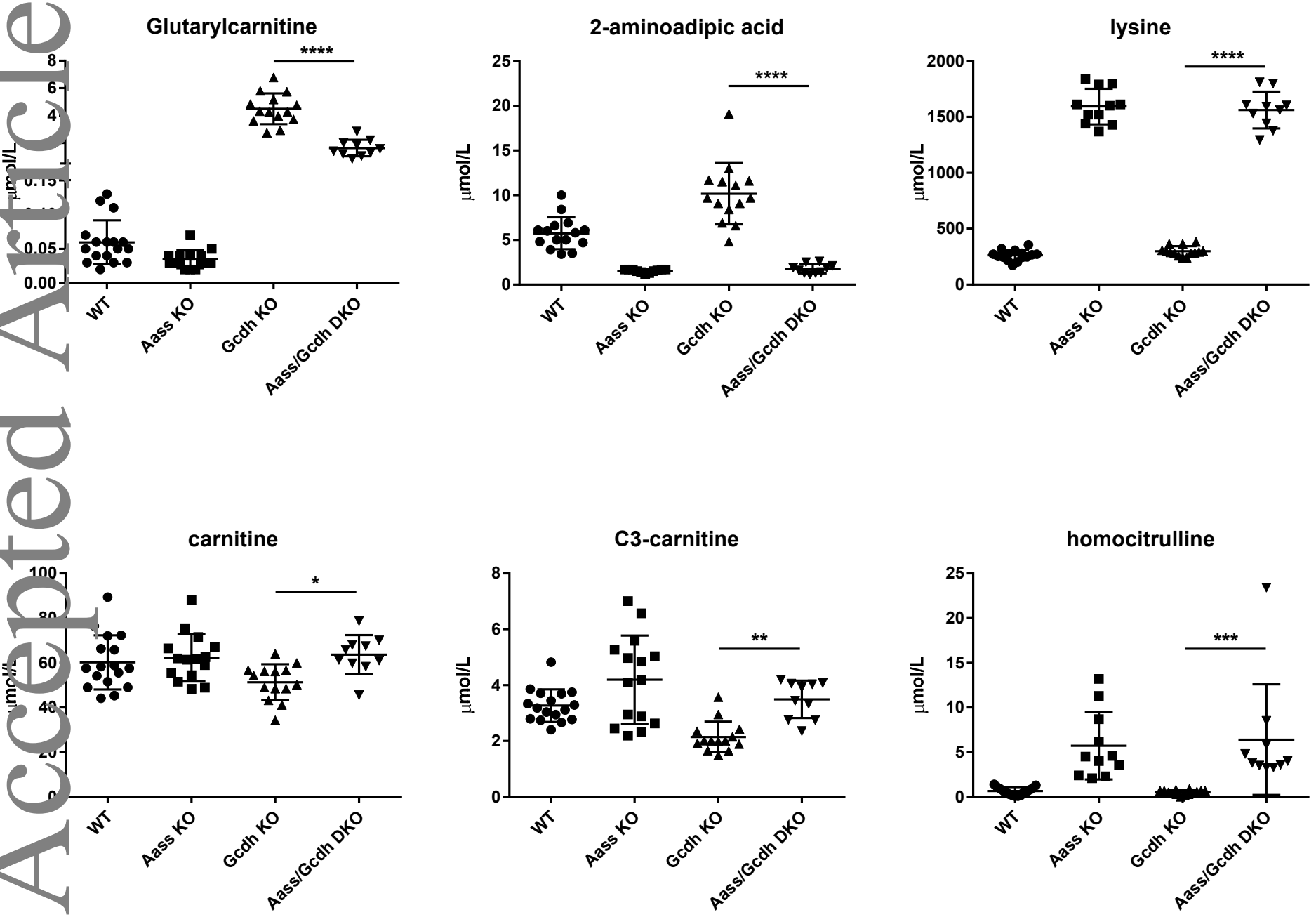

Figure 4